

Impact of thickness of liquid crystal layer on response rate and exponential gain coefficient with assistance of ZnSe film

Cuiling Meng, Hua Zhao, Tingyu Xue, Jiayin Fu, and Jingwen Zhang*

Department of Physics, Harbin Institute of Technology, Harbin 150001, China

*Corresponding author: jingwenz@gmail.com

Received 18 July 2014; revised 2 November 2014; accepted 6 November 2014;
posted 7 November 2014 (Doc. ID 217154); published 17 December 2014

A response time as short as 5.4 ms and an exponential gain coefficient as large as 1795.0 cm^{-1} were obtained in C_{60} doped 4,4'-*n*-pentylcyanobiphenyl liquid crystal cells sandwiched with two indium tin oxide glass plates coated with nanoscale photoconductive ZnSe films, which is believed to be facilitating charge-carrier generation and transportation and, hence, to be responsible for the fast response rate. The surface-mediated photorefractive effect and the ZnSe interlayers were both behind the high gain coefficients. The two-dimensional diffraction patterns observed in our system are also discussed. © 2014 Optical Society of America

OCIS codes: (090.0090) Holography; (090.5694) Real-time holography.
<http://dx.doi.org/10.1364/AO.53.008456>

1. Introduction

For decades, exploration of novel photorefractive (PR) materials and optimization of existing ones have not stopped attracting researchers [1,2]. Compared to inorganic materials such as LiNbO_3 , organic materials, including polymers [3,4] and liquid crystals (LCs) [5,6], occupy an important niche in holographic display owing to their high figures of merit, easy processing, and flexibility [7,8]. Also, the low dc voltage needed in LC devices [1,5] is highly desirable in real-world uses [4,7]. However, there is still much room for the improvement of response rate in LC-based holographic recording media. Since discovery of the PR effect in LCs [1], a considerable number of researchers have been continuously engaged in optimizing LC materials and structures of LC cells [9,10]. However, most reported PR-like effects in nematic LCs are slow in response rate [1,6] or transient in diffraction efficiency and energy transferring [11,12],

which hinder applicability of LCs in real-time holography and optical information processing.

By introducing photoconducting interlayers [11–17] into LC cells, response times as short as tens of ms have been achieved in the past years. Encouragingly, stable holographic grating can be written within 15.1 ms by introducing a photoconductive film between the LC layer and an indium tin oxide (ITO) electrode [5]. Along this line, it is natural to push the response rate higher to get over 100 frames/s by optimizing the structure of LC cells. When the thickness of the LC layer was varied, great improvements in response rate and exponential gain were seen. A response time as short as 5.4 ms was achieved, leading to practical, real-time holographic display, at least in terms of updatable recording. In addition, an exponential gain coefficient (EGC) as large as 1795.0 cm^{-1} was obtained from the thinnest LC cell with a $3.5 \mu\text{m}$ thick spacer. These results once again hint at a surface-dominating PR-like effect. Comparing the LC cells used in the research reported in this paper with conventional ones in most reported works, it can be inferred that the photoconductive

ZnSe interlayers play key roles in raising the response rate and the EGC.

2. Experimental

As stated in [3], photoinduced charge carrier generators, transporting agents, trapping sites, and optical nonlinear functionality are all necessary constituents for PR grating formation. In making specimens, (1) ZnSe was chosen to be a photoconductive agent, which is responsible mainly for the transporting of charge carriers and partially for their generating and trapping functionalities; (2) 4,4'-*n*-pentylcyanobiphenyl (5CB) was employed for its excellent nonlinearity, such as birefringence and photoelectric effect; and (3) fullerene C₆₀ was added to serve as efficient charge generators and partially as trapping agents due to its large triplet yield, broad absorption, and multiple stable reduced states [18,19].

The materials used in making LC cells, 5CB LC (Merck) and fullerene C₆₀ (Aldrich), are commercially available, an exception being the ZnSe thin films. We characterized the LC cells with different LC layer thicknesses ranging from 3.5 to 62.0 μm. Photoconductive ZnSe films (500 nm) were directly deposited on the top of two ITO glass plates with e-beam evaporation methodology (LJ-550E, LJ-UHV Technology Company). Fullerene C₆₀ was mixed with 5CB at a weight ratio of 0.05 weight % (wt.%). The surface area of the LC cells measure as 2.4 × 1.8 cm, with differing thicknesses of LC layer set by spacers. It should be emphasized that ZnSe films also serve as aligning layers, in addition to their role of charge-carrier transporting. In this way, the screening effect of an additional aligning layer to the dc field in conventional LC cells can be avoided. It should be mentioned here that the absorption coefficients of various specimens vary within a relatively small range, from 0.016 to 0.130 cm⁻¹. The schematic diagram of the structure of a typical LC cell and the experimental setup used in this work are shown in Fig. 1.

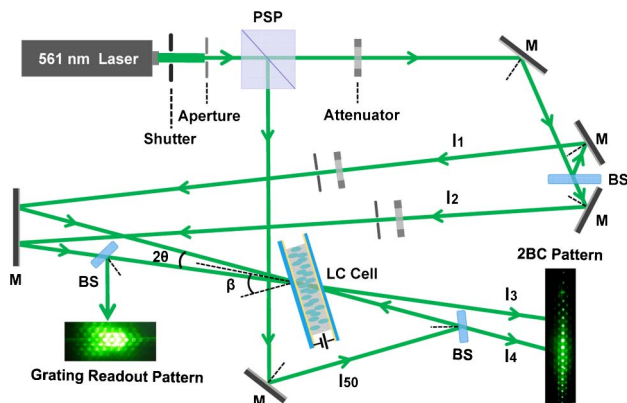


Fig. 1. Experimental configuration for two-beam coupling (2BC) measurements and diffraction efficiency with a probing beam propagating against one of the two recording beams. BS, beam splitter; M, mirror; PSP, polarization splitting prism.

A. Two Beam Coupling Experiments

With a typical slanted geometry like the one shown in Fig. 1, a semiconductor diode pumped laser with center wavelengths of 561.0 nm was used in performing 2BC experiments. The LC cell was tilted at an angle $\beta = 45^\circ$ to the bisector of two recording beams I_1 and I_2 , with a crossing angle at $2\theta = 1.0^\circ$ and corresponding grating spacing $\Lambda = 18.9 \mu\text{m}$. Two *p*-polarized recording beams, I_1 and I_2 , were tuned into equal intensity, $14.2 \text{ mW} \cdot \text{cm}^{-2}$, illuminating on the LC cell at an intersection of 0.07 cm^2 . However, the grating written by two *s*-polarized beams is very slight in strength since the director axis of LC molecules is always perpendicular to the electric field E . Thus, the rotative moment of a LC molecule, expressed as $\Gamma \propto (n \times E)(n \cdot E)$, would be equal to the zero vector. In addition, most obvious coupling happened in a case where two writing beams were tuned into equal intensity, because the contrast of interference fringe is the best for equal intensity. Consequently, this should lead to the best PR index modulation, i.e., the best PR grating.

Seven specimens with different thicknesses of the LC layer were fabricated, and EGCs versus applied voltages were measured. As shown in Fig. 2(a), the experimental results indicated a complicated process of space-charge field formation in LC cells with ZnSe interlayers. Besides the 3.5 and 5.1 μm thick specimens, the EGCs of the rest of the specimens fell within a relatively narrow range, from -540.1 to 161.2 cm^{-1} . However, a special feature was found in the 3.5 μm thick specimen. At first, the EGCs fell into a negative value briefly, and then jumped back to positive territory, charging up to the largest value of 1795.0 cm^{-1} , followed by a slow decreasing process, until 12.0 V applied voltage. Interestingly, the 5.1 μm thick specimen exhibited opposite behavior, which first climbed to positive territory, and then dropped down into -1031.5 cm^{-1} . Both reversed their coupling directions around 2.5 V, which can be illustrated well by the 2BC dynamics, as shown in Fig. 2(c). Here, the direction change of energy transferring probably stemmed from the space charge redistribution, which led to the phase shift between the total index refraction modulation and the interference pattern. At the same time, the standard deviation of the EGC became very large as voltage increased to 5.5–6.5 V. As the voltage increased further, the scattering of two transmitted beams intensified and gave rise to weaker energy coupling between the two main beams. In our work, EGCs were calculated according to $\Gamma = (\cos(\beta)/d) \ln(\gamma_0 \cdot \gamma_1)$, where γ_0 and γ_1 refer to the transmitted intensity ratio of two recording beams before and after applying a dc field, respectively. It is worth noting that precise EGCs cannot be measured through 2BC dynamics, shown in Fig. 2(b), in which values are not equal to the real intensities due to two attenuators and nonlinear amplifications of two photodiodes (used to detect I_3 and I_4). It should be noticed that although the detection system is nonlinear, the relation

between the values on the 2BC dynamics and real intensity is still monotonically increasing. The data shown in Fig. 2(a) were measured with a power meter (Thorlabs PM100D) for better precision.

Fig. 2(a) shows that decreasing thickness of the LC layer increased the absolute value of the EGCs. To get an in-depth understanding of this special feature of the EGCs, it is necessary to take surface-mediated effects into account. It was seen that when switching off the dc field, a temporary intensity increase was observed, followed by slowly decreasing [as shown in Fig. 2(c)]. If it is merely volume gratings that are responsible for the previously mentioned phenomenon, the intensity would disappear gradually because volume torque is proportional to the dc field. However, in the case of surface-mediated gratings, removing the dc field would lead to a temporary increase of the intensity because of the existence of an easy axis grating (at the beginning of the relaxation). In the meantime, the strength or the phase shift in this type of grating is only related to the LC/ZnSe interface. As a result, the net 2BC gains [calculated as $\cos(\beta) \ln(\gamma_0 \cdot \gamma_1)$] are comparable for various specimens [as seen from Fig. 2(b)] since they are mainly determined by the surface refractive index modulation. According to the definition of EGCs, the smaller the thickness d , the larger the EGCs [Fig. 2(a)]. As reported lately, the strong electrostatic modification in the LC/ZnSe interface might be responsible for the huge energy transferring between the laser beams involved [20]. In the relatively thin LC cells, the surface effect was even more dominating than that in the thicker ones. The surface plasmon polariton coupling with the diffraction light might be behind the direction change of the energy transferring, since excitation of surface plasmon polaritons, and their coupling with visible light, is very sensitive to a slight index refractive index change, and/or a phase change. Actually, the applied voltage of 2.5 V charged one of the ZnSe/LC interfaces with a high density of electrons, which can support surface plasmon polaritons. Once surface plasmon polaritons play roles in the energy coupling, the directional change of the energy transferring could be changed by an external stimulus. In fact, in this material

system, the physical processes involved are complicated and deserve further in-depth investigation. For the thicker specimens, the volume effect can average out the surface effect, and hence no obvious directional change of energy transferring was seen under the experimental conditions.

One can see more details of 2BC process in the 3.5 μm thick specimen from Fig. 2(c), in which the energy transferring was steady and no much transient portion was seen. It is also seen that considerable asymmetrical energy transferred from one beam to the other at a voltage over 2.0 V. Namely, the loss in one beam is more than the gain in the other. This indicates that the gratings written were surface-dominated, and partial energy was lost to the higher diffraction orders. Particularly, at 6.0 V, energy competition between two recording beams and scattering began to appear. However, the influence of the scattering is relatively weak at 6.0–6.5 V. Moreover, the attenuations of both beams were observed at 6.5 V, instead of amplification in one beam and attenuation in the other. This is due to diffraction to higher orders, seen in both sides. However, higher diffraction orders do not necessarily lead to a declining gain coefficient. On the one hand, the strength of grating also becomes stronger as the voltage increases. On the other hand, the very thin thickness of the LC layer (in the 3.5 μm specimen) is the main reason for the very large gain coefficient, as mentioned previously. It is also observed in the 2BC experiments that the higher the voltage that was applied, the more frequently power fluctuations were seen in both beams, indicating strong energy competitions among the main beams and different diffracted orders. This also explains why the standard deviations of gain coefficient were so large at 5.5–6.5 V, as shown in Fig. 2(a).

B. Grating-Probing Experiments

Response rate is crucial for monitoring grating formation and assessing the holographic performance of specimens, which can be measured by applying a counterpropagating beam. Previously, a response time of 15.1 ms was attained in a similar specimen with a grating spacing of 18.1 μm [5]. However, not

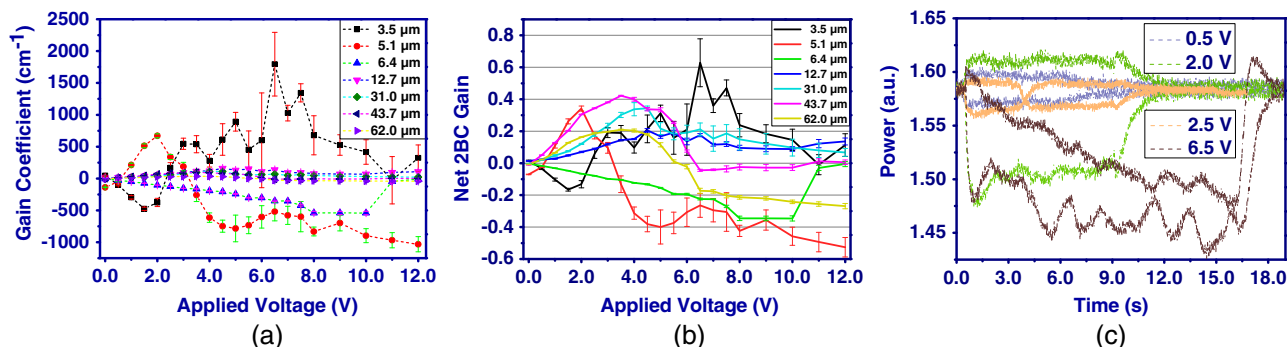


Fig. 2. (a) 2BC exponential gain coefficients versus applied voltages in the seven specimens (with different thicknesses of the LC layer). (b) Net 2BC gains versus applied voltage in the seven specimens. (c) Dynamic curves obtained at 0.5, 2.0, 2.5, and 6.5 V in a 3.5 μm thick LC cell.

much attention was paid to the detailed study of the influence of cell thickness on the response rate and diffraction efficiency. In addition, owing to the formation of a two-dimensional pattern observed in both 2BC and grating-probing experiments, we investigated the relationship between cell thickness and response performance.

Both *p*-polarized and *s*-polarized probing beams were employed to read out the PR gratings. An *s*-polarized beam was introduced by a polarization splitting prism, shown in Fig. 1, and it propagated precisely against one of the two recording beams. It is worth noting that all gratings recorded in this work fall into the Raman-Nath regime, in which many high diffraction orders are expected (as presented in Fig. 1). Intensity of the first non-Bragg orders was measured by a photodiode connected to a digital oscilloscope in demonstrating the response dynamic. In this work, a response time was defined as the interval from the turning on of the writing beams to the moment when the first-order diffractive beam reaches the value of $[1 - (1/e)] \times I_{\max}$, where I_{\max} is the maximum intensity of the first-order diffractive beam.

It can be seen from Fig. 3(a) that the response times of various gratings measured with an *s*-polarized reading beam were 20 ms faster than that with a *p*-polarized one, on average. This is reasonable since a *p*-polarized probing beam would interact with

the writing ones with the identical polarization. Consequently, this can smear out the existing gratings and write their own. However, an *s*-polarized probing beam can pass LC cells independent of the writing beam since their polarized directions were perpendicular to each other.

Although response under *s*-polarized probing has an advantage over *p*-polarization, there still is a similar trend in both *s*- and *p*-polarized probing cases. As the thicknesses of LC cells increase from 3.5 to 62.0 μm , the response time declined rapidly, and then increased slowly, with one minimum response time at 6.4 μm , as shown in Fig. 3(b). The only difference was that with *s*-polarized probing, the shortest response time of 5.0 ms was obtained in the 43.7 μm thick one. In spite of this, the first-order diffraction of the 6.4 μm thick specimen was more stable than that of the 43.7 μm thick one. It is worth noting that the diffraction efficiency and gain coefficient in the 6.4 μm thick specimen were relatively low, as shown in Fig. 3(c). Further improvement is definitely needed for practical applications. Regarding the fastest response obtained in the 6.4 μm thick specimen, there is no easy answer to the real reason owing to the complicated processes involved. Generally speaking, the response was determined by the surface and volume effects. The thinner a specimen, the less the freedom of the LC molecules within it. The thicker the specimen, the greater the contribution from the

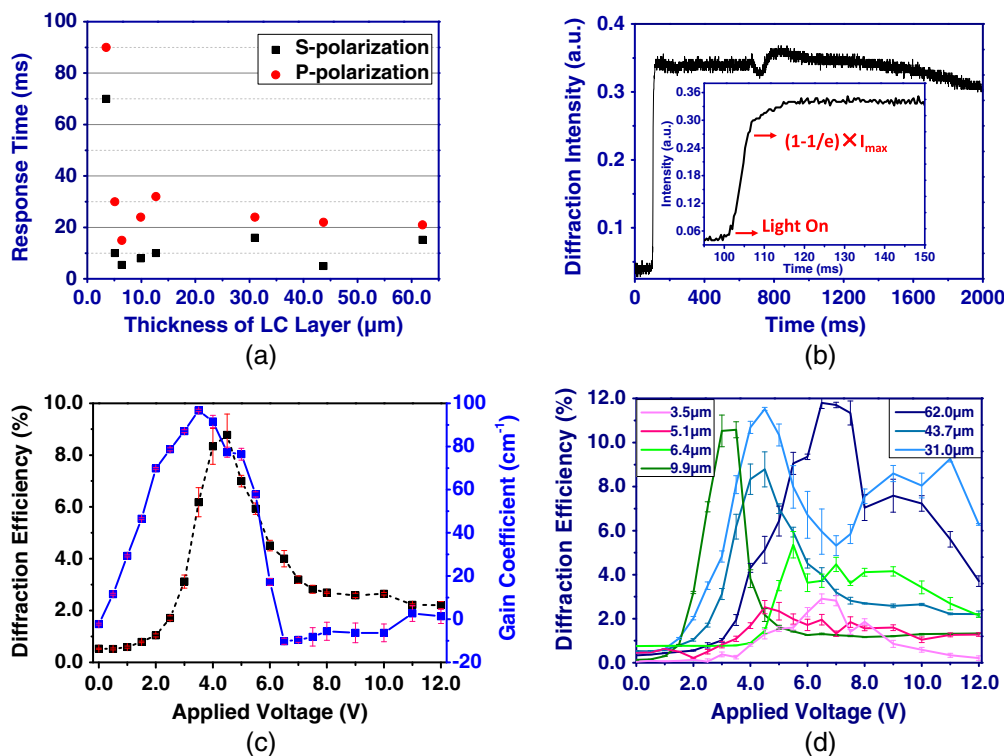


Fig. 3. (a) Response time of the first-order diffraction versus thickness of LC layers under *s*- and *p*-polarized probing beams at applied voltage of 11.0 V. (b) A typical response dynamic of the first-order diffractive beam of the 6.4 μm thick specimen under *s*-polarized probing beam at 11.0 V. The detailed response curve is indicated in the inset. (c) Diffraction efficiency/gain coefficient of the 6.4 μm thick specimen versus applied voltage at the same recording intensity obtained from the grating-probing and 2BC experiments, respectively. (d) First-order diffraction efficiency of seven specimens.

volume effect. The faster response of the surface effect in the thinner specimens can be compromised by the relatively low freedom of the LC molecules. Therefore, it is believed that the 6.4 μm thick specimen might happen to be in the optimal condition in our case. Further effort along this line will be put forth to get better and clearer answers and will be included in further publications.

More importantly, the grating formation process in our case is much faster than that reported in [21–23]. This result is promising in real-time holographic display, as the corresponding frame rate for 5.4 ms is comparable to modern display. By comparison, it was found that no grating was formed in LC cells without a ZnSe film, even when a quite high electric field was applied. This difference suggests that fast response rate is most probably attributable to the photoconductive ZnSe interlayer.

One notes that relatively low diffraction efficiencies were measured in the thinner specimens [Fig. 3(d)]. As discussed previously, the relatively low diffraction efficiency originates from the relatively small contribution from the volume effect. It is known that the amplitude of volume grating is proportional to the value of the diffraction efficiency [24], specifically to the first-order diffraction.

It is widely proved that introducing photoconductive materials can facilitate both the modulation of surface charge and the formation of a space charge field through the prevention of ion injection from the ITO layer into the PR film. In our case, the key to boosting response performance lies in the fast excitation of charge carriers within the interference pattern by virtue of the ZnSe film, owing to fast mobility of charge carriers (mainly electrons). To attain a faster response, grating space and concentration of 5CB to C₆₀ have to be considered simultaneously.

In addition, the photoconductivity properties of ZnSe can be excited at 0.59–0.65 eV with a Zn:Se ratio from 0.2:1 to 1:1, which indicates that LC cell depositing ZnSe can work in an IR waveband. Hence, introducing ZnSe as substrates of a nematic LC cell would expand its applications to an IR waveband. Moreover, the fastest response rate measured in a

LC layer of 6.4 μm is closely consistent with that of a commercial LC display.

C. Two-Dimensional Patterns in Both 2BC and Grating-Probing Experiments

Intriguingly, two-dimensional patterns were observed in both the grating writing and probing experiments. Pattern formation in nonequilibrium systems is one of the most intriguing topics in science. In the past, a number of nonlinear optical materials have been proved to be excellent media for the study of pattern formation, including LCs [25], organic films, and atomic vapor [26,27]. Owing to intense inherent instabilities, exhibiting pattern formation in nonlinear media by two counterpropagating beams was dominant in most reported systems [25–30]. However, the difference in our cases is that pattern formation was observed by two copropagating beams. That is, it is transmission grating, rather than refraction grating, that supported pattern formation.

As shown in Fig. 1, beams I_1 and I_2 were incident upon the LC cell from one side simultaneously. 2BC and grating-probing patterns were also presented in Fig. 1. These patterns were very different from those seen in most cases, where only one-dimensional diffraction patterns were observed. These special patterns deserve further exploration on the gratings written.

The distance for observing patterns in our case was more than 2.0 m and met the condition $z \geq (1/2\lambda)(x_0^2 + y_0^2)_{\text{max}}$, where $\lambda = 561.0 \text{ nm}$ and $x_{0 \text{ max}} = y_{0 \text{ max}} = 0.15 \text{ cm}$. Hence, the diffractions belong to the Fraunhofer diffraction, in which diffraction aperture (PR grating) and diffraction field meet the Fourier transform relationship. That is, the inverse Fourier transform of the pattern corresponds to the grating morphology. Accordingly, the grating morphology was tentatively calculated and is presented in Fig. 4. The left column signifies the original diffraction patterns at 0, 3.0, and 5.0 V in the grating-probing experiment; the middle column shows the inverse Fourier transforms of the corresponding patterns; and the right column represents the norms of the inverse Fourier transforms. It can be seen from

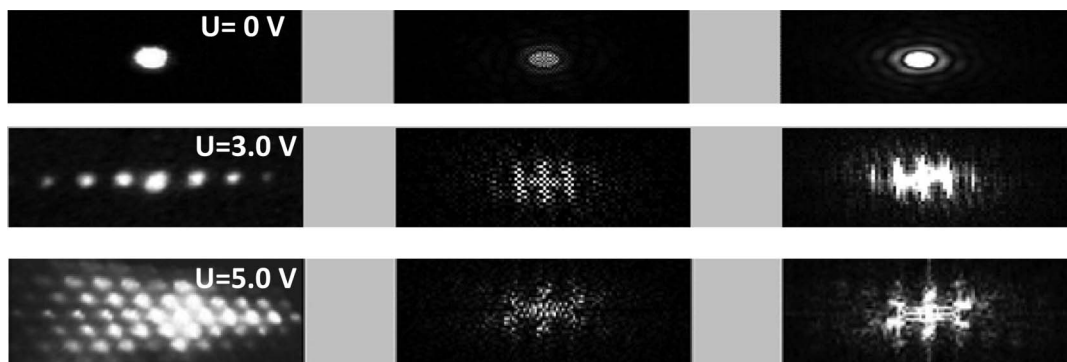


Fig. 4. Diffraction patterns and their Fourier transforms. The left column is the grating-probing patterns observed at 0, 3.0, and 5.0 V. Their corresponding Fourier transforms and the norms of the Fourier transforms are presented in the middle and right columns, respectively.

the left column that as voltage increased, the probing beam gradually transformed from a spot to one-dimensional spots and, finally, to a two-dimensional pattern. At the same time, the grating formed in a LC cell extended from one spot to a one-dimensional grating, and then to a hexagonal pattern, which was similar with the filamentation of a single beam [31]. It should be noticed that such a two-dimensional pattern was obtained just in a 31.0 μm thick specimen. The reason why a two-dimensional pattern appeared, and only in 31.0 μm , must be explored further.

Owing to the complicated energy transferring direction changes in two-beam coupling, apparent surface dominating PR gratings, and two-dimensional pattern formation, it is natural to turn attention toward the interface of ZnSe/LC. Actually, the semi-conducting ZnSe layers can be modified by charge accumulation upon applying an electric field. The charge density of the very thin layer of ZnSe, adjacent to the LC, can be raised greatly by charge carrier accumulation; this change should contribute to the complicated phenomena seen in this work. Intensive research along this line is still ongoing.

3. Conclusion

In conclusion, holographic performance was investigated in C_{60} doped 5CB LC cells sandwiched between two ITO glass plates coated with ZnSe films. An EGC as high as 1795.0 cm^{-1} was obtained in the cell with a 3.5 μm LC layer at 6.5 V. The large gain coefficient was tentatively attributed to the surface-mediated PR effect. More importantly, real-time hologram writing time of 5.4 ms and stable diffraction were obtained in the specimen with a 6.4 μm thick LC layer at 11.0 V. The excellent charge carrier generation and transportation in ZnSe are believed to be the main reasons for the fast response. The experimental results obtained were a further step toward a real-time holographic display. Moreover, low activation energy of ZnSe makes it possible to operate the specimens in an IR waveband. In addition, two-dimensional patterns observed in both 2BC and grating-probing experiments were studied preliminarily.

This work has been supported by a grant from the National Natural Science Foundation of China under project no. 11174067. The authors are indebted to the Key Laboratory of Micro-Optics and Photonics Technology of Heilongjiang Province, Harbin, China, for full access to the facility.

References

1. I. C. Khoo, H. Li, and Y. Liang, "Observation of orientational photorefractive effects in nematic liquid crystal," *Opt. Lett.* **19**, 1723–1725 (1994).
2. H. Zhao, C. Lian, X. Sun, and J. W. Zhang, "Nanoscale interlayer that raises response rate in photorefractive liquid crystal polymer composites," *Opt. Express* **19**, 12496–12502 (2011).
3. O. Ostroverkhova and W. E. Moerner, "Organic photorefractives: mechanisms, materials, and applications," *Chem. Rev.* **104**, 3267–3314 (2004).

4. S. Tay, P.-A. Blanche, R. Voorakaranam, A. V. Tunc, W. Lin, S. Rokutanda, T. Gu, D. Flores, P. Wang, G. Li, P. St. Hilaire, J. Thomas, R. A. Norwood, M. Yamamoto, and N. Peyghambarian, "An updatable holographic three-dimensional display," *Nature* **451**, 694–698 (2008).
5. H. Zhao, C. Lian, F. Huang, T. Xue, X. Sun, and J. W. Zhang, "Impact of grating spacing and electric field on real time updatable holographic recording in nanoscale ZnSe film assisted liquid crystal cells," *Appl. Phys. Lett.* **101**, 211118 (2012).
6. F. Simoni and L. Lucchetti, "Photorefractive effects in liquid crystals," in *Photorefractive Materials and Their Applications 2*, P. Günter and J.-P. Huignard, eds. (Springer, 2007), pp. 571–605.
7. P.-A. Blanche, A. Bablumian, R. Voorakaranam, C. Christenson, W. Lin, T. Gu, D. Flores, P. Wang, W.-Y. Hsieh, M. Kathaperumal, B. Rachwal, O. Siddiqui, J. Thomas, R. A. Norwood, M. Yamamoto, and N. Peyghambarian, "Holographic three-dimensional telepresence using large-area photorefractive polymer," *Nature* **468**, 80–83 (2010).
8. J. Zhang, V. Ostroverkhov, K. D. Singer, V. Reshetnyak, and Yu. Reznikov, "Electrically controlled surface diffraction gratings in nematic liquid crystals," *Opt. Lett.* **25**, 414–416 (2000).
9. I. C. Khoo, "Nonlinear optics of liquid crystalline materials," *Phys. Rep.* **471**, 221–267 (2009).
10. S. Bartkiewicz, A. Miniewicz, B. Sahraoui, and F. Kajzar, "Dynamic charge-carrier-mobility-mediated holography in thin layers of photoconducting polymers," *Appl. Phys. Lett.* **81**, 3705–3707 (2002).
11. I. C. Khoo, "The infrared optical nonlinearities of nematic liquid crystals and novel two-wave mixing processes," *J. Mod. Opt.* **37**, 1801–1813 (1990).
12. H. Ono and N. Kawatsuki, "Orientational holographic grating observed in liquid crystals sandwiched with photoconductive polymer films," *Appl. Phys. Lett.* **71**, 1162–1164 (1997).
13. I. Gvozdosky, K. Shcherbin, D. R. Evans, and G. Cook, "Infrared sensitive liquid crystal photorefractive hybrid cell with semiconductor substrates," *Appl. Phys. B* **104**, 883–886 (2011).
14. A. Miniewicz, S. Bartkiewicz, A. Januszko, and J. Parka, "Nematic liquid crystals as media for real-time holography," *J. Incl. Pheno. Macro. Chem.* **35**, 317–325 (1999).
15. J. Mysliwiec, A. Miniewicz, and S. Bartkiewicz, "Influence of light on self-diffraction process in liquid crystal cells with photoconducting polymeric layers," *Opto-Electron. Rev.* **10**, 53–58 (2002).
16. B. Sahraoui, I. Fuks-Janczarek, S. Bartkiewicz, K. Matczyszyn, J. Mysliwiec, I. V. Kityk, J. Berdowski, E. Allard, and J. Cousseau, "Enhancement of third-order optical susceptibility of C_{60} -TTF compounds using nematic liquid crystal," *Chem. Phys. Lett.* **365**, 327–332 (2002).
17. C. Lian, H. Zhao, Y. Pei, X. Sun, and J. Zhang, "Fast response beam coupling in liquid crystal cells sandwiched between ZnSe substrates," *Opt. Express* **20**, 15843–15852 (2012).
18. S. M. Silence, C. A. Walsh, J. C. Scott, and W. E. Moerner, "C60 sensitization of a photorefractive polymer," *Appl. Phys. Lett.* **61**, 2967–2969 (1992).
19. Y. Zhang, Y. P. Cui, and P. N. Prasad, "Observation of photorefractivity in a fullerene-doped polymer composite," *Phys. Rev. B* **46**, 9900–9902 (1992).
20. T. Xue, H. Zhao, C. Meng, J. Fu, and J. Zhang, "Impact of surface plasmon polaritons on photorefractive effect in dye doped liquid crystal cells with ZnSe interlayers," *Opt. Express* **22**, 20964–20972 (2014).
21. K. S. Jang, H. M. Yang, J. Kim, and J. D. Kim, "Dynamic formation of diffraction grating in a photorefractive liquid crystal cell with mesoporous TiO_2 layers," *IEEE Trans. Nanotechnol.* **7**, 115–119 (2008).
22. X. Sun, F. Yao, Y. Pei, and J. Zhang, "Light controlled diffraction gratings in C_{60} -doped nematic liquid crystals," *J. Appl. Phys.* **102**, 013104 (2007).
23. M. Tamburrini, M. Bonavita, S. Wabnitz, and E. Santamato, "Hexagonally patterned beam filamentation in a thin liquid-crystal film with a single feedback mirror," *Opt. Lett.* **18**, 855–857 (1993).

24. A. Sobolewska and A. Miniewicz, "Analysis of the kinetics of different efficiency during the holographic grating recording in azobenzene functionalized polymers," *J. Phys. Chem. B* **111**, 1536–1544 (2007).
25. X. Sun, Y. Pei, F. Yao, J. Zhang, and C. Hou, "Optical amplification in multilayer photorefractive liquid crystal films," *Appl. Phys. Lett.* **90**, 201115 (2007).
26. G. Grynberg, A. Maitre, and A. Petrossian, "Flowerlike patterns generated by a laser beam transmitted through a rubidium cell with single feedback mirror," *Phys. Rev. Lett.* **72**, 2379–2382 (1994).
27. T. Ackemann and W. Lange, "Non- and nearly hexagonal patterns in sodium vapor generated by single-mirror feedback," *Phys. Rev. A* **50**, R4468 (1994).
28. W. J. Firth and A. Fitzgerald, "Transverse instabilities due to counterpropagation in Kerr media," *J. Opt. Soc. Am. B* **7**, 1087–1097 (1990).
29. R. Neubecker, G. L. Oppo, B. Thuring, and T. Tschudi, "Pattern formation in a liquid-crystal light valve with feedback, including polarization, saturation, and internal threshold effects," *Phys. Rev. A* **52**, 791–808 (1995).
30. T. Honda, "Hexagonal pattern formation due to counterpropagation in KNbO₃," *Opt. Lett.* **18**, 598–600 (1993).
31. A. V. Mamaev, M. Saffman, D. Z. Anderson, and A. A. Zozulya, "Propagation of light beams in anisotropic nonlinear media: from symmetry breaking to spatial turbulence," *Phys. Rev. A* **54**, 870–879 (1996).